Electrotactile Feedback Improves Grip Force Control and Enables Object Stiffness Recognition While Using a Myoelectric Hand

Guohong Chai, *Member, IEEE*, Han Wang, *Student Member, IEEE*, Guangye Li, *Member, IEEE*, Xinjun Sheng, *Member, IEEE*, and Xiangyang Zhu, *Member, IEEE*

***Abstract*—Current myoelectric hands are limited in their ability to provide effective sensory feedback to the users, which highly affects their functionality and utility. Although the sensory information of a myoelectric hand can be acquired with equipped sensors, transforming the sensory signals into effective tactile sensations on users for functional tasks is a largely unsolved challenge. The purpose of this study aims to demonstrate that electrotactile feedback of the grip force improves the sensorimotor control of a myoelectric hand and enables object stiffness recognition. The grip force of a sensorized myoelectric hand was delivered to its users via electrotactile stimulation based on four kinds of typical encoding strategies, including graded (G), linear amplitude (LA), linear frequency (LF), and biomimetic (B) modulation. Object stiffness was encoded with the change of electrotactile sensations triggered by final grip force, as the prosthesis grasped the objects. Ten able-bodied subjects and two transradial amputees were recruited to participate in a dual-task virtual eggs test (VET) and an object stiffness discrimination test (OSDT) to quantify the prosthesis users' ability to handle fragile objects and recognize object stiffnesses, respectively. The quantified results showed that with electrotactile feedback enabled, the four kinds of encoding strategies allowed subjects to better able to handle fragile objects with similar performance, and the subjects were able to differentiate four levels of object stiffness at favorable accuracies (>86%) and high manual efficiency. Strategy LA presented the best stiffness discrimination performance, while strategy B was able to reduce the discrimination time but the discrimination accuracy was not better than the other three strategies. Electrotactile feedback also enhanced prosthesis embodiment and improved the users' confidence in prosthetic control. Outcomes indicate electrotactile feedback can be effectively exploited by the prosthesis users for grip force control and object stiffness recognition, proving the feasibility of functional sensory restoration of myoelectric prostheses equipped with electrotactile feedback.**

***Index Terms*—Myoelectric hand, electrotactile feedback, grip force, stiffness recognition, transradial amputees.**

Manuscript received December 18, 2021; revised April 13, 2022; accepted May 3, 2022. Date of publication May 9, 2022; date of current version May 26, 2022. This work was supported in part by the China National Key Research and Development Program under Grant 2018YFB1307200, in part by the National Natural Science Foundation of China under Grant 51805320 and Grant 91948302, and in part by the China Postdoctoral Science Foundation under Grant 2019M651504 and Grant 2020T130409. *(Corresponding author: Xiangyang Zhu.)*

This work involved human subjects or animals in its research. Approval of all ethical and experimental procedures and protocols was granted by the Ethics Committee of Human and Animal Experiments of Shanghai Jiao Tong University, China.

Guohong Chai is with the State Key Laboratory of Mechanical System and Vibration, School of Mechanical Engineering, and the Meta Robotics Institute, Shanghai Jiao Tong University, Shanghai 200240, China, and also with the Cixi Institute of Biomedical Engineering, Ningbo Institute of Materials Technology and Engineering, Chinese Academy of Sciences, Ningbo, Zhejiang 315211, China (e-mail: ghchai99@nimte.ac.cn).

Han Wang, Guangye Li, Xinjun Sheng, and Xiangyang Zhu are with the State Key Laboratory of Mechanical System and Vibration, School of Mechanical Engineering, and the Meta Robotics Institute, Shanghai Jiao Tong University, Shanghai 200240, China (e-mail: mexyzhu@sjtu.edu.cn).

Digital Object Identifier 10.1109/TNSRE.2022.3173329

I. Introduction

HAND amputation deprives the motor and sensory functions in upper-limb amputees. An acceptable level of grasping function can be regained by translating residual muscle electrical activity into the commands of the motorized myoelectric hands via multi-channel surface electromyography (sEMG) control interfaces [1], [2]. However, the advanced myoelectric hands are frequently abandoned or rejected by amputees, and lack of tactile feedback has been identified as one of the major drawbacks [3], [4]. To date, except few recent examples with a limited clinical application [5], [6], no commercially-available myoelectric hands can provide effective tactile feedback for amputees to close the control loop. It has been confirmed that providing tactile feedback can not only improve the controllability [6], [7] and enhance the sense of embodiment of myoelectric hands [8], [9], but also can reduce amputee users' phantom limb pain [9], [10]. Restoration of tactile feedback may potentially improve the functionality and utility of myoelectric hands, thereby decreasing the abandon rate [11].

Tactile sensory feedback plays an irreplaceable role when humans interact with external surroundings [5], [6], [12]. It enables grip force control [13]–[15], and allows us to detect object physical properties (e.g., object size/stiffness, texture, etc.), with or without visual feedback [7], [16]–[22]. The appropriate grip force is critical for delicate grasping and reliable object handling (e.g., avoid slip or crush of a fragile object) since it cannot be directly adjusted by means

This work is licensed under a Creative Commons Attribution-NonCommercial-NoDerivatives 4.0 License.
For more information, see https://creativecommons.org/licenses/by-nc-nd/4.0/

of vision [23]. However, for upper-limb amputees, myoelectric control of grip force of a prosthetic hand in a graded manner (i.e., gradually change grip force) is a rather difficult task due to the deprivation of physiological structures [24], [25]. He/she has to re-learn how to grade force output based on indirect or substituted somatosensory feedback [26]. Artificial tactile feedback, even non modality-matched (e.g., vibratory cues), can contribute to the grip force control and motor coordination [14], [15], [27], [28]. Previous studies have shown that when performing a delicate manipulating task (e.g., VET), invasive tactile feedback could improve the performance of grip force control even accompanied by a parallel cognitive task (e.g., handling fragile objects while memorizing numbers) [7], [14], [29]. Nevertheless, the invasive tactile feedback is still limited to the stage of amputee case studies because of the uncertainties of surgery and potential risks (e.g., post-surgery care, long-term stability of microelectrodes or biocompatibility, etc. [5], [17]). Hence, it is essential to study that whether non-invasive tactile feedback can be effectively used for the grip force control of a myoelectric hand, since so far it has not been quantitatively evaluated by prosthesis users [29].

Additionally, stiffness is an important object feature that cannot be reliably identified via visual feedback alone [30]–[32]. Object stiffness recognition has been evaluated using various non-invasive [16], [17], [33] or invasive stimulation approaches [7], [18], [19]. Most of the closed-loop feedback studies adopted the linear modulation of one kinds of stimulation parameters (e.g., change of the current amplitude) as a function of the prosthesis sensor readouts (e.g., grip force or aperture angle) to transmit object stiffness [7], [17]–[19], [29], [34]. Some recent related studies proposed that several non-linear biomimetic encoding strategies were able to enhance the recognition performance (e.g., better selectivity or shorter identification time, etc.) [7], [35]. But on the whole, stiffness recognition is assessed largely based on invasive stimulation approaches. The adopted object stiffness is usually no more than three levels and the recognition accuracies vary greatly among different encoding strategies [16], [19]. Therefore, inspired by these studies on stiffness recognition, here we also want to investigate whether the objects with more than three stiffness levels can be effectively distinguished via non-invasive stimulation approaches. This is important and meaningful to the functional sensory restoration of myoelectric hands in practice.

Electrotactile stimulation is widely applied for sensory restoration of prosthetic hands due to the obvious advantages, such as non-invasive, decoupled parameters, compact electronics with a different number and arrangement of electrode pads [5], [6], [12]. In the present study, we hypothesize that the electrotactile feedback can effectively improve the users' ability in regulating the grip force and enabling object stiffness recognition. To this aim, four kinds of typical (G, LA, LF and B modulation) encoding strategies were adopted to convey the grip force from the prosthetic hand to its users in the form of electrotactile feedback. We carried out a dual-task VET [27] and an OSDT [36], [37] to evaluate the both kinds of functional performance of the myoelectric hand, respectively. The utility of electrotactile feedback and the prosthesis embodiment were also surveyed through a questionnaire. The current findings provide important insights into the non-invasive sensory restoration of myoelectric hands, and have the potential to be directly applied to commercial prosthetic hands.

TABLE I
INFORMATION OF THE TWO TRANSRADIAL AMPUTEES

Subjects(gender, age, handedness)	Amputation side,cause and since time (years)	Prosthetic type, prosthetic usage and stump length (cm)[a]
A1 (F, 63, right)	Left, trauma, 34	All day, cosmetic, 19
A2 (M, 40, right)	Right, trauma, 13	All day, myoelectric, 15

[a]Stump length refers to distance from elbow crease to stump terminal.

II. MATERIALS AND METHODS

A. Subjects

Ten healthy, able-bodied subjects (age 22-32 years, two females, all right-handed) and two unilateral transradial amputees (see Table I) participated in the study. All experiments were conducted in accordance with the declaration of Helsinki and approved by the Ethics Committee of Human and Animal Experiments of Shanghai Jiao Tong University, Shanghai, China. All subjects were informed about the experimental procedure and signed the informed consent forms prior to participation.

B. Experimental Setup

A bidirectional hand prosthesis system was developed for this study. We instrumented a single degree of freedom (S-DOF) myoelectric hand (SJQ18, Danyang Prostheses Factory, Co., Ltd., China) with low-profile force sensitive resistors (Flexi-Force A101; Tekscan, Inc., America) mounted on the pads of the thumb and index fingers of the prosthesis. A rotation angle sensor (SV01A103AEA01R00, Murata Manufacturing Co., Ltd., Japan) was immobilized at the little finger edge of the prosthesis to measure the real-time aperture angle of the hand, where the inner rotation part of the angle sensor was mortise-tenon jointed with the rotational axis and the outer part was immobilized on the fixing parts of the prosthesis. We calibrated the pressure sensors with known weights. We calibrated the angle sensor by having the subject close the prosthetic hand to fixed apertures. The myoelectric hand was controlled by a proportional EMG controller with a couple of sEMG electrodes. Two sEMG electrodes provided the linear envelopes of the EMG signals which were processed by the EMG controller to control the grasping velocity of the robotic hand (proportional control). The electrode gain was set so that the signal generated during maximum voluntary contraction (MVC) fluctuated around the saturation level, 5% and 50% of MVC was linearly mapped with the normalized myoelectric signal (prosthesis input) between 0 and 1, respectively.

During a grasping movement, both real-time position and the contact pressure information of the prosthetic hand was simultaneously recorded via the two types of sensors and was

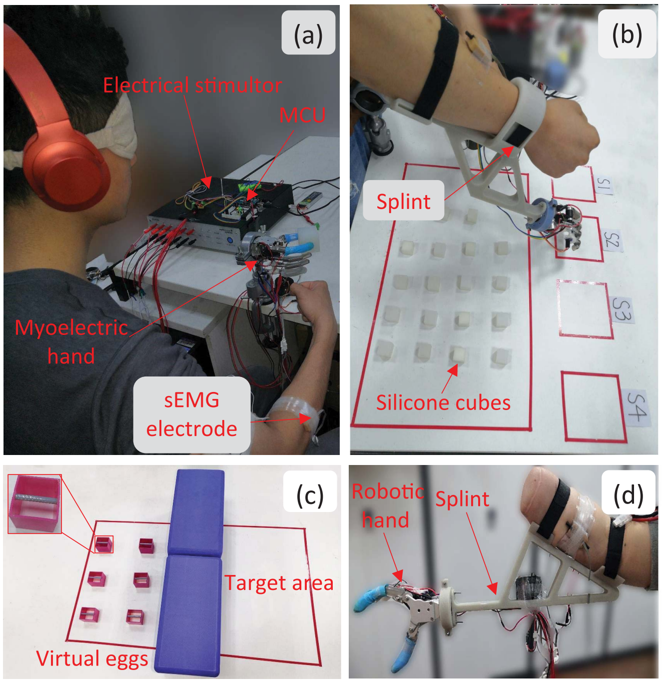

Fig. 1. Experimental setup and test objects. (a) Bidirectional myoelectric hand system stabilized on a table for object stiffness identification. (b) Performing object stiffness discrimination by controlling the robotic hand via a custom-designed splint (able-bodied subject). (c) Fragile blocks (virtual eggs) and the transfer-area. (d) Illustration of the robotic hand worn by amputee 1 via a custom-designed splint.

sent to a Micro Control Unit (MCU) (Arduino Mega2560) to trigger an electric stimulator (STG4008, GmbH, Germany), outputting the stimulation pulses to human skin areas through surface electrodes. The MCU control was implemented by calling the stimulation paradigm that was determined through psychophysical experiments [41], [42], pre-programmed and saved (in the form of stimulation parameters, including current amplitude, pule width and frequency) in the electrical stimulator through its programmable function. The bidirectional myoelectric hand could be stabilized on a table (at a fixed angle using a universal rotary fixing clamp) or worn by able-bodied and amputee subjects via a custom-designed splint that allowed them to maneuver the robotic hand with their arms/stumps, used for various functional tasks, as shown in Fig. 1(b) and 1(d).

C. Electrotactile Feedback

In current study, only the grip force between thumb and index fingers of the myoelectric hand was transmitted to its users in the form of electrotactile feedback. We delivered biphasic, charge-balanced, cathode-first electrical pulses to targeted skin area via a pair of non-woven stimulation electrodes (12mm in diameter) which were connected to the anode/cathode of one channel of the stimulator. To convey effective electrotactile feedback, based on prior studies [7], [18], [35], four kinds of typical encoding strategies were proposed to deliver the grip force as follows: 1) *Graded (G) modulation*. In this strategy, the stimulation was fixed at the four sets of optimal stimulation parameters [(3mA, 200μs, 10Hz), (3mA, 250μs, 25Hz), (3mA, 160μs, 100Hz), and (3mA, 300μs, 150Hz)] which could be as constant values for all subjects to elicit four levels of distinguishable tactile (vibration/pressure) sensations to deliver the grip force. The full force range of the myoelectric hand was divided into four sub-ranges (ranges 1-4, corresponding to the four levels of object stiffness, sorted in ascending intensity order) through a pretest with the given test objects. 2) *Linear amplitude/frequency (LA/LF) modulation*. Two kinds of linear encoding algorithms were proposed. i.e., the stimulation amplitude and frequency increased solely on the basis of the absolute sensor value. 3) *Biomimetic (B) modulation*. The biomimetic algorithm was developed and modified from literature [7]. Both the stimulation frequency and amplitude increased together on the basis of the absolute sensor value and on positive rate of change of the sensor. Stimulation intensity tracked the current sensor value plus 3 times any positive finite difference between the current and previous sensor values. All encoding algorithms and the corresponding stimulation parameters were determined through a prior test using the method of limits [38], shown in Table II.

D. Experimental Protocols

The whole experiment consisted of the pilot and formal experiments. The pilot experiment aimed to determine the optimal encoding parameters, train the subject to correctly identify the electrotactile feedback and familiarize with the prosthesis control. For all subjects, in order to avoid mutual interference, the sEMG electrodes and the stimulation electrodes were separately placed on the forearm (dominant hand for able-bodied subjects, and residual stump for amputees) and outside of the contralateral upper arm (about 6cm above the elbow crease), respectively. A pair of antagonistic (wrist flexor/extensor) muscles were used to control the robotic hand, and the optimal positions on the forearm were determined with palpation. Before mounting the electrodes, all targeted skin areas were cleaned with alcohol pads to remove dirties and skin debris, to acquire high-quality electrotactile sensations. Due to different subjects had different sensitivity, thus, under the pre-defined stimulation parameters (Table II), the final parameters were then fine-tuned to assure that each subject could clearly perceive the optimal electrotactile sensations on the selected feedback sites within respective tests. When the encoding parameters were determined, the subjects started the training task. The electrotactile codes (force/stiffness level) were randomly presented, and the subject was asked to identify the feedback information associated with the delivered codes. The experimenter provided verbal feedback in respect to the correct identification (reinforced learning). As soon as the subject could correctly recognized all pre-set codes twice in a row (around 2-3min for each subject), the training stopped. Afterwards, the principle of prosthesis operation and the experimental procedures were explained and the subject briefly practiced (3-5 *min*) controlling the prosthesis, and started the formal experiment.

The formal experiment included a dual-task VET and an OSDT. In each task, four forms of tactile feedback were separately provided to the subjects based on four kinds of

TABLE II
ENCODING ALGORITHMS AND STIMULATION PARAMETERS USED FOR ELECTROTACTILE FEEDBACK

Encoding algorithm(s)	Analytic formulation[a]	Stimulation parameters		
		Amplitude (mA)	Pulse Width (μs)	Frequency (Hz)
Graded	A_t=A_i; P_t=P_i; F_t=F_i; i=1, 2, 3, 4	3/3/3/3	200/250/160/300	10/25/100/150
Linear amplitude	A_t=c_t(A_{max}-A_{min})+A_{min}	1.5–5	200	50
Linear frequency	F_t=c_t(F_{max}-F_{min})+F_{min}	3	200	1-120
Biomimetic	$A_t = \begin{cases} c_t(A_{max} - A_{min}) + A_{min} & v_t < 0 \\ (3v_t + c_t) * (A_{max} - A_{min}) + A_{min} & v_t \geq 0 \end{cases}$ $F_t = \begin{cases} c_t(F_{max} - F_{min}) + F_{min} & v_t < 0 \\ (3v_t + c_t) * (F_{max} - F_{min}) + F_{min} & v_t \geq 0 \end{cases}$	1.5-5	200	1-120

[a]A_t, P_t and F_t are the stimulation amplitude, pulse width, and frequency at time *t*, respectively; v_t is velocity of the robotic hand at time *t*; c_t is the normalized contact value at time *t*, where, c_t = current sensor value / (sensor value$_{max}$ - sensor value$_{min}$). Note that the tactile feedback is off and no stimulation occurs when c_t = 0.

encoding strategies. Before the test of each encoding strategy, all subjects performed a short training session (1-2 min) to become accustomed to the respective task.

In the VET, the subjects, wearing the myoelectric hand, were instructed to transfer the fragile blocks presented in front of he/her from one side to the other over a 15cm-tall wall as quickly as possible and without breaking them within one minute (see Fig. 1(c)), timed using a chronometer. The virtual eggs (40 $\times$ 40 $\times$ 40 mm^3 plastic blocks equipped with a mechanical fuse (L = 39mm, d = 2.5mm, weight $\approx$ 25g) perched on two opposite walls via two concave holes, 80g) would break when grasped with a grip force (perpendicular to the mechanical fuse main axis) larger than 16$\pm$0.7N (N = 50, about 8mm/s grip force), which was determined through a repeated test in advance. The VET performance was evaluated on four kinds of feedback conditions [only visual feedback (V), visual + distraction task (V+D), visual + tactile feedback (V+T) and visual + distraction task + tactile feedback (V+D+T)]. The performance was measured by the number of transferred (broken and unbroken) blocks and the percentage of the transferred unbroken blocks over the total transferred blocks. During the distraction task, a verbal counting task was performed alongside the VET, the subject was required to skip-count backwards by twos (e.g., 100, 98, 96, 94…) in an even tone from a chosen number (between 100 and 90, given by the experimenter), at approximately the rate of one digit per second. For every subject, there were 10 repetitions in each feedback condition, and each condition was performed in a pseudo-random order.

In the OSDT, object stiffness was encoded with the electrotactile sensations elicited by the final grip force, as the prosthesis grasped the objects. Considering that a direct control of the prosthetic hand also can provide users with additional information (e.g., contact pressure from prosthetic socket, etc) [5], [6], we performed two variants of OSDT to evaluate the stiffness recognition performance. In the first variant, all subjects were instructed to perform an off-prosthetic stiffness recognition task (OSRT). Both the visual and auditory cues were isolated with a sleep mask and a pair of noise-canceling headphones playing gray noise (Fig. 1(a)). The subjects, seated in a chair but not wore the robotic hand, were required to control the myoelectric hand to discriminate four deformable blocks (20 cm^3 white silicone cubes, casted with hydrogels) of different stiffness (20A, 40A, 60A and 80A in durometer) by the delivered electrotactile feedback. Once the subject could recognize the presented object stiffness, he/she pressed a press-button to stop the electrotactile feedback, and then reported the answer to the experimenter, which also made the laptop record the subject's identification time (from robotic hand contacting the target object). For every subject, each cube was presented 10 times by the experimenter in a balanced, pseudo-randomized order for each form of electrotactile feedback. In the second variant, all subjects were instructed to perform a block-foraging stiffness discrimination task (BSDT) [36], [37]. Five each of the four kinds of white silicone blocks (cannot be discriminated by the appearance) were randomly placed on a rectangular area (30cm*25cm) of the experimental table (Fig. 1(b)). The subjects, wearing the myoelectric hand, were informed to discriminate and transfer them into four target classified-areas (10cm*10cm) within participants' reach, according to the respective stiffness as soon as possible through electrotactile feedback. Once the subjects completed the discrimination task, the discrimination time was recorded by the experimenter by clicking another press-button. To reduce auditory and mitigate possible visual cues (such as, material compressibility or sheen), all subjects wore a pair of noise-canceling headphones playing gray noise, and a frosted glasses across the second variant. There were 10 repetitions on every subject for each form of electrotactile feedback in the BSDT. All repetitions were performed in a pseudo-random order across all subjects and encoding strategies. After the BSDT, each subject was also instructed to performed a baseline trial three times where 20 of the cubes was randomly divided into 5 each, and move them into the four target classified-areas without tactile feedback. We measured the stiffness recognition performance with the correct identification/discrimination rate (*CIR*/*CDR*) and the identification/discrimination time.

During the experiment, the breaks of 1-5 minutes were randomly given between two feedback conditions, to allow the subjects to relax and also avoid the adaptation of electrotactile stimulation and the muscle fatigue (used for sEMG control). The duration of the overall experiment was about 4-4.5 hours for each subject.

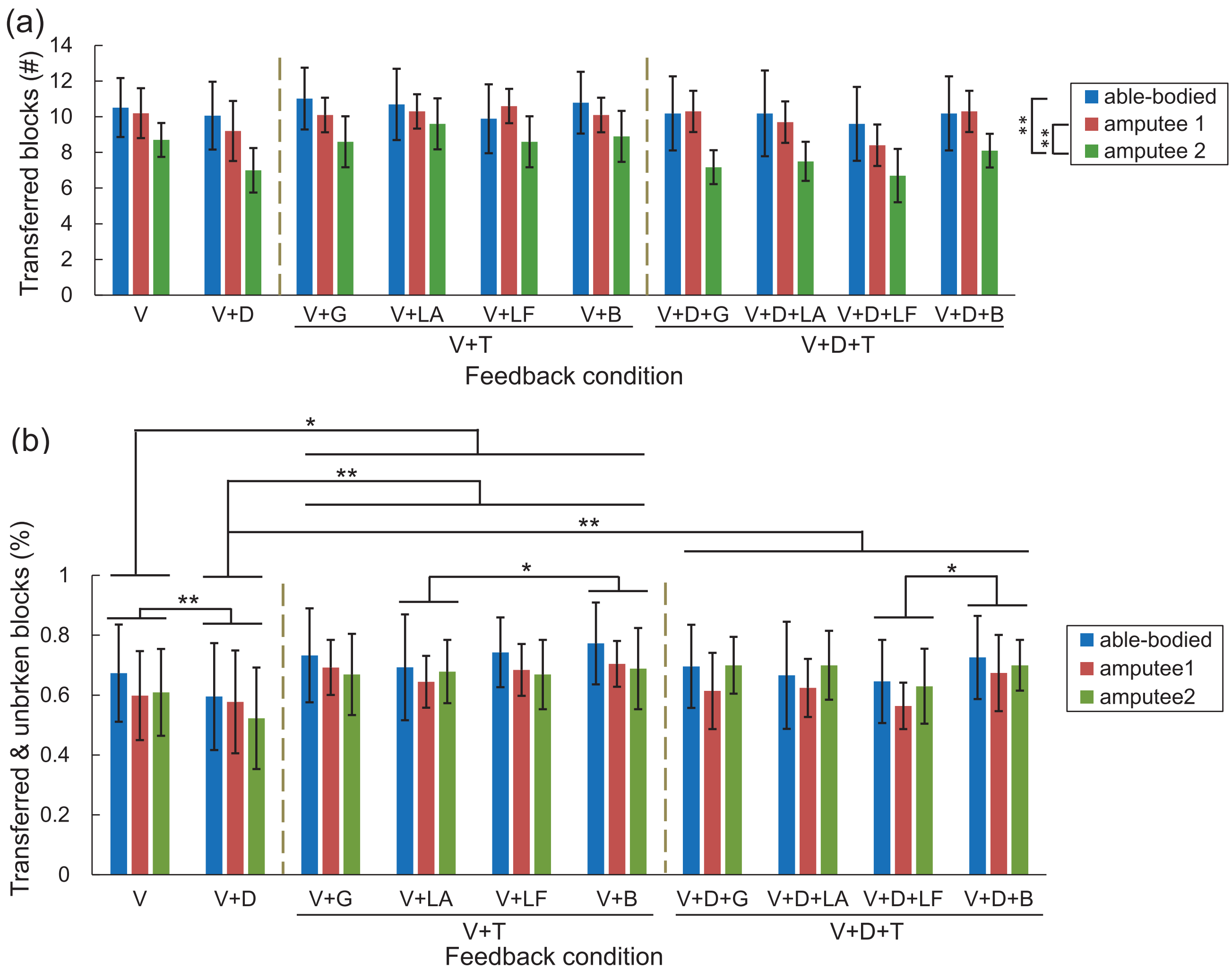

Fig. 2. Dual-task virtual eggs test (VET) with different forms of tactile (graded-G, liner amplitude-LA, liner frequency-LF and biomimetic-B) feedback. (a) Numbers of the transferred blocks on four kinds of feedback conditions (V, V+D, V+T, V+D+T). (b) Percentages of the unbroken blocks over the transferred blocks. V, D and T represent the visual feedback, distraction (skip-counting) task and tactile feedback, respectively. Symbols * and ** indicate significant differences with a level of ($p < 0.01$) and ($p < 0.05$), respectively.

E. Psycho-Physiological Assessments

After the experiment, we asked every subject to rate his/her confidence in his/her ability to perform the VET and OSDT, on a scale of 0-10. In additional, all subjects were asked to complete a brief evaluation questionnaire. The questions probed the usefulness of electrotactile feedback in the daily functional activities, whether it elicited or enhanced a sense of embodiment of the prosthetic hand, psychological burden, deficiencies and suggestions for improvements.

F. Statistical Analysis

All data were analyzed using IBM SPSS STATISTICS 23.0. Statistical tests (Kolmogorov-Smirnov) indicated that the data were not normally distributed and therefore non-parametric tests (cruskal-wallis rank sum tests) were employed to evaluate the statistically significant differences. For VET and OSDT, Kruskal-Wallis H test was adopted to measure the significant influences of the subject type (able-bodied, amputee), encoding strategy (G, LA, LF and B) and feedback condition (V, V+D, V+T and V+D+T) on the numbers of the transferred (broken and unbroken) blocks or the *CIR*s/*CDR*s of blocks and identification/discrimination time, respectively. A further pairwise comparison was measured with Nemenyi test (coding rank method) when requested. Moreover, for a certain factor (subject type or feedback condition), Mann-Whitney U test was used to further examine the intra-group significance of the dependent variables if necessary. A *p*-value less than 0.05 was considered statistically significant.

III. Results

A. Dual-Task Virtual Eggs Test (VET)

Fig. 2(a) shows the results of the transferred blocks on four kinds of feedback conditions (V, V+D, V+T, V+D+T). For able-bodied subjects and amputees 1 and 2, the Kruskal-Wallis H test showed that there were no significant differences of the transferred blocks among the conditions V (11±2, 10±1 and 9±1), V+D (10±2, 10±2 and 7±1), V+G (11±2, 10±1 and 9±1), V+LA (11±2, 10±1 and 10±1), V+LF (10±2,

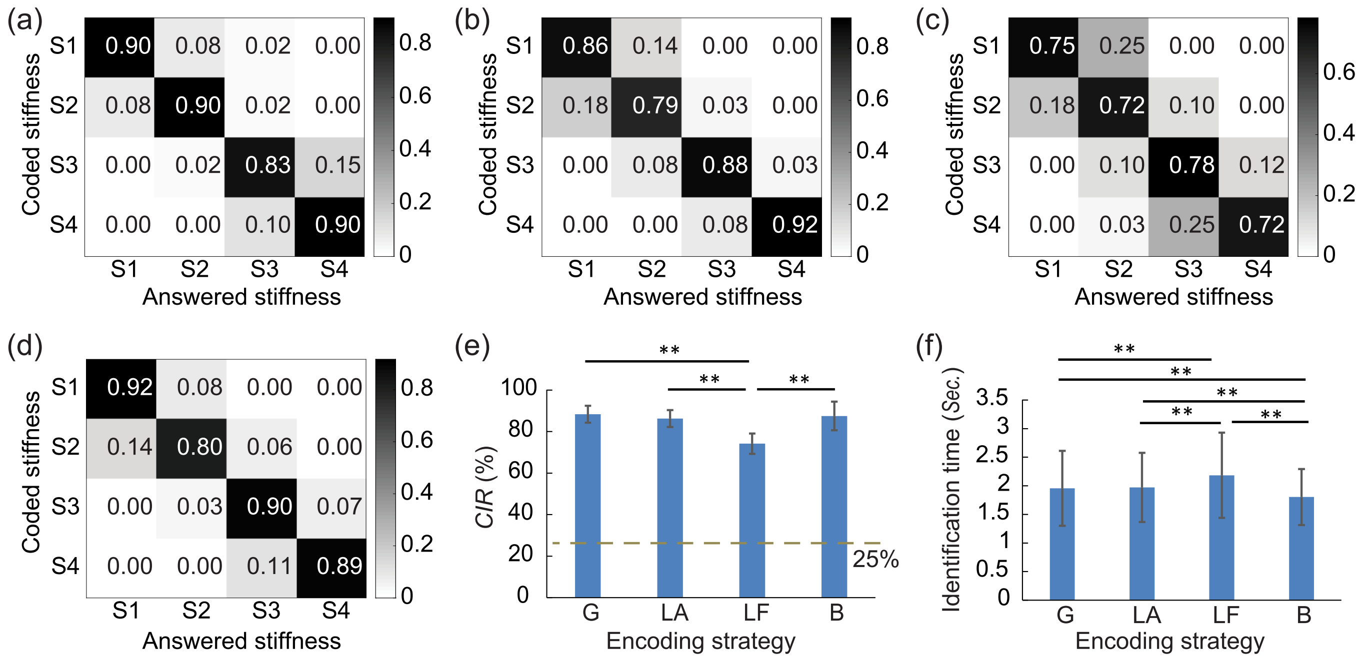

Fig. 3. Confusion matrices quantifying the object stiffness recognition across all subjects using encoding strategies G (a), LA (b), LF (c) and B (d). (e) Average *CID*s with the standard errors (S.E.) and (f) Average identification time with the standard errors (S.E.) based on four kinds of encoding strategies. Horizontal grey dashed line indicates the chance level (25%). S1 to S4 represent the stiffness levels from soft to hard, respectively. All the acronyms and symbols are the same as those in Fig. 2.

11±1 and 9±1), V+B (11±2, 10±1 and 9±1), V+D+G (10±2, 10±1 and 7±1), V+D+LA (10±2, 10±1 and 8±1), V+D+LF (10±2, 8±1 and 7±1) and V+D+B (10±2, 10±1 and 8±1), respectively. Both the able-bodied subjects and amputee 1 did not show significant difference, while the amputee 2 had the relatively less transferred blocks in respective feedback conditions.

Fig. 2(b) shows the percentages of the unbroken blocks over the transferred blocks on four kinds of feedback conditions (V, V+D, V+T, V+D+T). For able-bodied subjects, amputees 1 and 2, the percentages of the unbroken blocks (67.3%±16.2%, 59.8%±14.9% and 60.9%±14.5%) on condition V were significantly higher than those (59.5%±17.9%, 57.1%±19.2% and 52.3%±17.0%) on condition V+D, but obviously lower than those [V+G (73.3%±15.7%, 69.2%±9.1% and 66.8%±13.6%), V+LA (69.3%±17.7%, 64.4%±8.7% and 67.9%±10.6%), V+LF (74.3%±11.7%, 68.4%±8.7% and 66.9%±11.6%) and V+B (77.3%±15.7%, 70.4%±7.7% and 68.9%±13.6%)] on condition V+T. The percentages of the unbroken blocks [V+D+G (69.6%±13.9%, 61.4%±12.7% and 70.0%±9.5%), V+D+LA (66.6%±17.9%, 62.4%±9.7% and 70.0%±11.5%), V+D+LF (64.6%±13.9%, 56.4%±7.7% and 63.0%±12.5%) and V+D+B (72.6%±13.9%, 67.4%±12.7% and 70.0%±8.5%)] were not evidently reduced by the distraction task when the electrotactile feedback was provided (V+D+T). The Kruskal-Wallis H test showed that there were no significant differences among the able-bodied subjects and two amputees, respectively. Mann-Whitney U tests indicated that within conditions V+T and V+D+T, no significant differences were displayed among the four forms of tactile feedback with the exceptions of two pairwise comparisons (V+LA versus V+B, V+D+LF versus V+D+B).

B. Object Stiffness Discrimination Test (OSDT)

1) Off-Prosthetic Stiffness Recognition: Kruskal-Wallis H test showed no significant difference was found between the able-bodied subjects and two amputees. The stiffness recognition accuracies across all subjects based on four kinds of encoding strategies were presented in Fig. 3(a)-3(e). The results showed that four kinds of encoding strategies led to similar performance in stiffness recognition. Specifically, with strategies G, LA, LF and B, the subjects were able to correctly identify the four types of object stiffness with an average *CIR* of 88.3%±4.1%, 86.3%±4.1%, 74.2%±4.9% and 87.5%±6.9%, respectively. The confusion matrices (Fig. 3(a)-3(d)) illustrated that the types of errors were largely composed of incorrect identification of adjacent stiffness levels. The four kinds of encoding strategies were found to be evidently greater than the chance value ($p < 0.001$), and the average *CIR* based on strategy LF was significantly lower than those with the other three kinds of strategies ($p < 0.01$) (Fig. 3(e)).

The identification time for four types of object stiffness was showed in Fig. 3(f). For strategies G, LA, LF and B, the average identification time was 1.9s±0.7s, 2.0s±0.6s, 2.2s±0.8s and 1.8s±0.5s, respectively. The Kruskal-Wallis H test showed that there were significantly differences among the four kinds of strategies except an pairwise comparison between the strategies G and LA ($p < 0.01$).

2) Block-Foraging Stiffness Discrimination: The *CDR*s for 20 cubes with four types of stiffness based on the four kinds of encoding strategies were quantified on able-bodied subjects (Fig. 4(a)) and two amputees (Fig. 4(b)), respectively. The results showed that the majority of the cubes were able to be correctly discriminated by the different stiffness. Specifically,

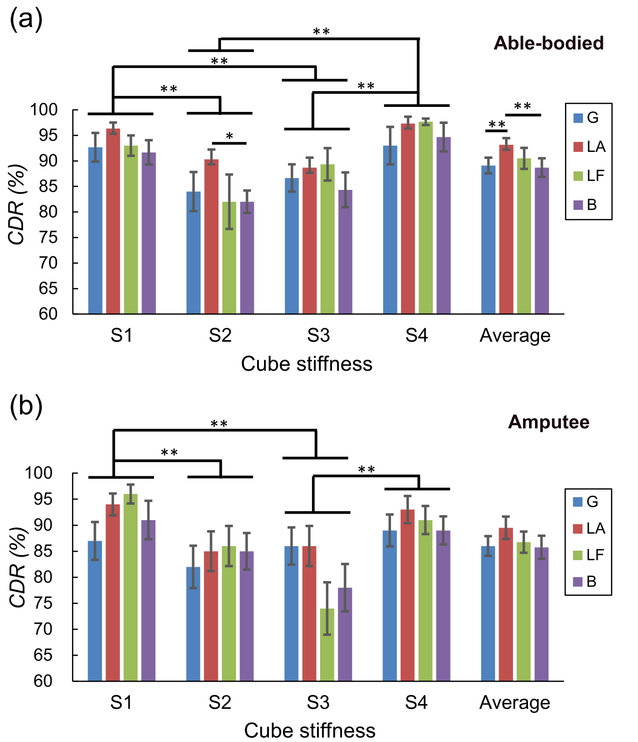

Fig. 4. Block-foraging stiffness discrimination based on four kinds of encoding strategies (G, LA, LF and B). Correct discrimination rates (*CDR*s) for 20 cubes with four types of stiffness on (a) able-bodied subjects and (b) two amputees. All the acronyms and symbols are the same as those in Fig. 2 and Fig. 3.

for able-bodied subjects, 20 cubes were correctly discriminated based on strategies G, LA, LF and B, resulting in an accuracy of 89.1%±1.6%, 93.2%±1.3%, 90.5%±2.1% and 88.7%±1.8%, respectively. Kruskal-Wallis H test showed that the *CDR*s based on strategy LA was significantly higher than those with the strategies G and B. Similarly, for two amputee subjects, the 20 cubes were correctly discriminated based on strategies G, LA, LF and B, resulting in an accuracy of 86.0%±1.9%, 89.5%±2.1%, 86.8%±2.0% and 85.8%±2.2%, respectively. Overall, for both able-bodied and amputee subjects, the softest (S1) and the hardest (S4) cubes were significantly easier to be discriminated than the two types of cubes with medium stiffness levels (S2 and S3), based on the four kinds of encoding strategies ($p < 0.001$). Mann-Whitney U tests showed that the significant difference was only found between able-bodied subjects and amputee 2 ($p < 0.01$).

The results of the discrimination time for BSDT comparable to random discrimination time are showed in Fig. 5. Based on strategies G, LA, LF and B, the discrimination times were 1.49±0.38 min, 1.36±0.24 min, 1.37±0.19 min and 1.29±0.19 min on able-bodied subjects, and 1.71±0.28 min, 1.55±0.23 min, 1.46±0.15 min and 1.34±0.18 min on amputees, respectively. As the control grasp, the random discrimination times were 0.85±0.19 min on able-bodied subjects and 0.91±0.22 min on amputees, respectively. Kruskal-Wallis H tests showed that there were significant differences between strategy G and the other three kinds of encoding strategies (G versus LA, G versus LF, G versus B) ($p < 0.01$) or the two types of subjects (able-bodied versus amputee) ($p < 0.01$), respectively. The stiffness discrimination times based on four kinds of encoding strategies were significantly longer than the respective random discrimination times ($p < 0.001$).

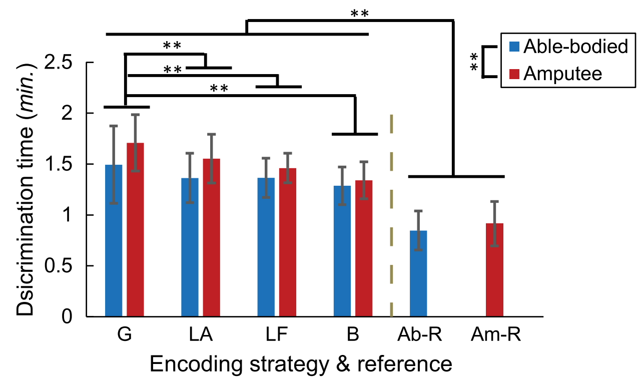

Fig. 5. Discrimination time for 20 cubes with baseline comparison of random discrimination time (Ab-R and Am-R). Ab-R and Am-R represent the random discrimination time averaged on able-bodied subjects and amputees, respectively. All other acronyms and symbols are the same as those in Fig. 4.

Trends of the *CDR*s and the discrimination time across all subjects over sequential number of trials are showed in Fig. 6(a) and Fig. 6(b), respectively. It was observed that for encoding strategies G, LA, LF and B, there was a consistent improvement of the *CDR*s in the first 3 trials, but no obvious learning effect was appeared in the subsequent discrimination trials. Accordingly, four kinds of the discrimination time had consistent rapid-decreasing phases from the 1st to the 3rd trial, and then entered the relative-steady phases in the follow-up trials, respectively. Kruskal-Wallis H tests indicated that no significant differences of the *CDR*s were found among the four kinds of encoding strategies, while the identification time based on strategy G was significantly longer than that with strategy B over sequential number of trials ($p < 0.01$).

C. Evaluation of Questionnaire

Fig. 7 shows the results of self-confidence scores regarding VET and BSDT. In the VET, the self-confidence results were presented based on different feedback conditions due to no significant differences were further found among the different forms of electrotactile (G, LA, LF and B) feedback. The self-confidence score (8.0±1.3) in performing the task with tactile feedback (V+T) was higher than that (7.0±1.2) without tactile feedback (V) and that (6.9±1.4) with tactile feedback and distraction task (V+T+D). By comparison, the self-confidence score was the lowest (5.6±1.3) when dual-task was performed without tactile feedback (V+D). Kruskal-Wallis H test showed that the significant differences of self-confidence score were found between the feedback condition V+D and the other three conditions (V versus V+D, $p < 0.05$; V+D versus V+T, $p < 0.01$; V+D versus V+T+D, $p < 0.05$), respectively. In the BSDT, based on encoding strategies G, LA, LF and B, the self-confidence scores were 7.2±0.8, 8.5±0.5, 6.7±1.5 and 8.1±1.0, respectively. Kruskal-Wallis H test showed that the significant differences were displayed between the strategies G and B ($p < 0.05$), LA and LF ($p < 0.05$), LF and B ($p < 0.05$), respectively.

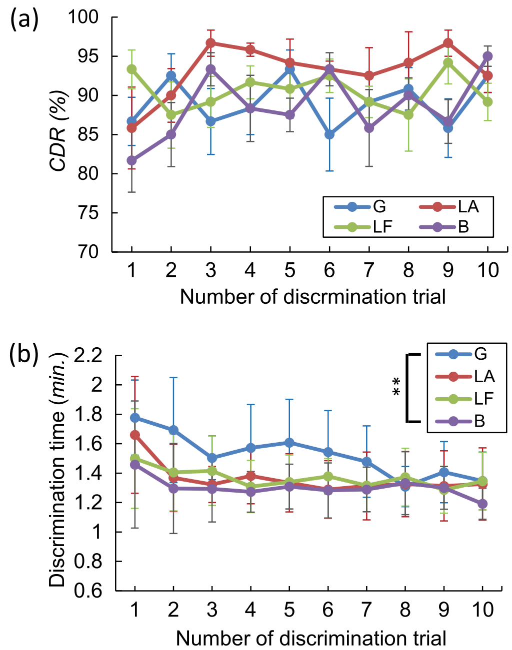

Fig. 6. Trends of (a) the *CDR*s and (b) the discrimination time over sequential number of discrimination trials. Error bars represented the standard errors (S.E.), averaged across all subjects in respective sequential number of trials. All acronyms and symbols are the same as those in Fig. 4 and Fig. 5.

Furthermore, all subjects reported that electrotactile feedback could highly reduce their dependence on visual feedback and increase the embodiment of the myoelectric hand. All subjects expressed that the current electrotactile feedback could be easily integrated into the sensorimotor control, applied for fragile object handling and object stiffness recognition. Ten subjects [except two able-bodied subjects, (10/12)] stated that current electrotactile feedback aroused an acceptable psychological burden, and they (9/12) agreed that the abandon rate of myoelectric hands could be potentially decreased if current electrotactile feedback could integrate with commercial myoelectric hands.

IV. Discussion

This study sought to demonstrate that electrotactile feedback could effectively improve grip force control of a myoelectric hand and enable the users to recognize object stiffness. The experimental results revealed that the four kinds of encoding strategies allowed the subjects to better able to handle fragile objects and discriminate four levels of object stiffness at favorable accuracies and high manual efficiency. To the best of our knowledge, it is the first time to quantify the users' ability in controlling a myoelectric hand to perform fragile object handling and object stiffness recognition through electrotactile feedback. These outcomes suggest the feasibility of electrotactile feedback being used for functional sensory restoration of myoelectric hands.

A. Electrotactile Feedback Improves Grip Force Control

Providing a tactile sensory feedback from a sensorized myoelectric hand, while performing a delicate manipulating task (e.g., VET), could help the amputees to regulate the grip force [14], [15], [27]. Based on consistent myoelectric control accuracy, how to transform the contact force into effective tactile cues (sensations) on the users is the key to fragile object handling. In the current VET, the quantified results (Fig. 2(b)) displayed that both able-bodied and amputee subjects were unable to effectively regulate the grip force relying on visual feedback when an alongside cognitive task (skip-counting numbers) was conducted simultaneously. As expected, based on the four forms of electrotactile feedback, the handling performance (percentage of unbroken blocks) could be significantly improved to comparable accuracies in both single-task (V and V+T) and dual-task (V+D, V+D+T), while maintaining similar efficiency (total number of transferred blocks, shown in Fig. 2(a)). The overall handling performance obtained based on electrotactile feedback (V+T: 69.8%; V+T+D: 67.1%) was equivalent to previous results reported in the literatures (about 70% in one or two amputees) using intraneural tactile feedback [7], [14], [29], [35]. This observation denotes that electrotactile feedback of grip force could be an effective alternative for transferring of fragile objects of the myoelectric hand. The relatively high self-confidences scores may help explain the plausibility, particularly in the dual-task (Fig. 7).

Specifically, both in single- and dual-tasks, no significant differences of the handling performance were displayed among the encoding strategies G, LA and LF. Whereas, the performance based on strategy B was superior than those with strategies G, LA and LF despite significant differences were only showed among partial strategies (see Fig. 2(b)). This means that the strategy B leading to a stronger stimulation (faster rate of the change of electrotactile intensity) during the contact transients can augment the improvements of the grip force control, which is in line with previous invasive studies [7], [35]. Therefore, we speculate that determining suitable stimulation parameters to elicit distinct electrotactile cues is crucial to the fragile object handling. Yet, more specific experiments with strategies G, LA and LF are needed to confirm it. Although the latest studies showed that the handling performance with electrotactile feedback was inferior than that with invasive feedback [14], and easier to be distracted by a parallel cognitive task (e.g, Span Digit Forward Test [39]) [29], this could be a pending question due to the delicate handling task was highly associated with myoelectric control, difficulties of the functional and parallel cognitive tasks [7], [14], [35], and individual differences, etc. Further contrast experiments are still necessary to investigate these discrepancies.

B. Electrotactile Feedback Enables Object Stiffness Recognition

Prior studies have shown that when grasping deformable objects, the rate of change of the grip force imposed on the object surface carried stiffness information, and the peak stimulation intensity/frequency sensed by the skin could be used for stiffness recognition [7], [18], [21]. Based on certain hand prosthesis system, stiffness recognition accuracy was mainly determined by the users' ability to discriminate the

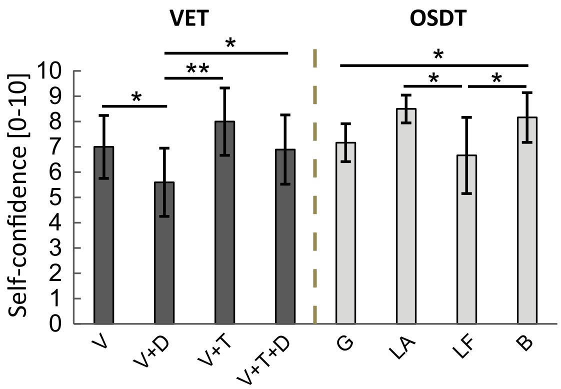

Fig. 7. Self-confidence scores in VET and OSDT under different feedback conditions (V, V+D, V+T and V+T+D) and based on different encoding strategies (G, LA, LF and B), separately. Each score was averaged across all subjects. All acronyms and symbols were the same as those in Fig. 2 and Fig. 4.

referred electrotactile sensations [18], [35]. In the OSRT, subjects' ability to stiffness discrimination was exclusively assessed based on electrotactile feedback without additional information during sensorimotor integration. The quantified results demonstrated that four forms of electrotactile feedback enabled the subjects to fairly identify four levels of common object stiffnesses at acceptable accuracies (84.1% on average) and efficiencies ($\leq$2.0s) [Fig. 3(e)-3(f)]. These accuracies were slightly higher or comparable with the results reported in previous studies (about 60% - 85% for three kinds of stiffness levels in one or two amputees) using intraneural tactile feedback through similar encoding strategies [35], [40], [41]. This indicates that electrotactile feedback is able to be exploited effectively to discriminate object stiffness with more than three levels. Differences in discrimination accuracy may be caused by multiple factors because of different encoding strategies. First, the differentiable stiffness levels and the discrimination accuracy are directly related to the ranges of allowable stimulation parameters. As the ranges of allowable parameters (e.g., current amplitude) for electrotactile feedback increases due to its non-invasiveness (see Table II), the number of distinct sensations, determined by the just-noticeable differences (JND), increases as well, thereby enhancing the distinguishability of objects with similar stiffness levels. This has been proved in previous literature through strategy LA [17]. By contrast, strategy LF enabled relatively lower recognition accuracy (74.2%) and longer identification time (2.2s). It might be that the subjects were less sensitive to the quick changes of frequency subranges of the four levels of stiffness due to fast-adaptation phenomenon of strategy LF, which also was found in intraneural sensory feedback [41]. Thus, how to transmit the electrotactile feedback using strategy LA to improve stiffness recognition performance will need to be investigated with further experiments. Overall, although strategy B enabled the subjects to identify the stiffness levels faster than with the other nonbiomimetic counterparts (Fig. 3(f)), no significant differences of the recognition accuracies were displayed among strategies G, LA and B. This may be due to the OSRT is not challenging enough to detect the performance differences.

Furthermore, we demonstrated that the ability to accurately distinguish object stiffness through electrotactile feedback could be translated into high performance during a daily BSDT with a direct control of the myoelectric hand. Based on the four kinds of encoding strategies, both able-bodied and amputee users could correctively discriminate the 20 deformable objects with four levels of common stiffness at favorable (>86%) accuracies (Fig. 4) and discrimination time [around 1.45min (4.4s for each object)] (Fig. 5), despite this task being impossible to achieve without tactile feedback. Specifically, the hardest and the softest objects were significantly easier to be discriminated than the intermediate hard objects, as a result of different object stiffnesses were sequentially encoded with a proportional intensity/frequency changes of electrotactile feedback [18]. Taking strategy G as a baseline, the overall discrimination accuracies demonstrated that linear amplitude (LA) modulation may be the most appropriate strategy for object stiffness discrimination when the stiffness levels were more than three (Fig. 4(a)). Instead, the biomimetic feedback was unable to evidently improve stiffness discrimination accuracy despite the discrimination efficiency could be highly improved (Fig. 4(a) and 4(b)). The most likely reason is that the bursts of the stimulation intensity during the contact transients might disturb or decrease the intensity discriminability of the bilinear changes of electrotactile sensations. Interestingly, the discrimination accuracy based on strategy LF was even higher than those with graded and biomimetic (G and B) feedback. It indicates that different stiffnesses are able to be effectively transferred to the subjects through linear frequency modulation, which can be explained that no obvious fast-adaptation is generated in the BSDT as long as the sequential stiffnesses are delivered with sufficient interval time. Meanwhile, the average discrimination time with strategy G was significantly longer than those based on the strategies LA, LF and B, while no significant differences were found among them (Fig. 5). It probably that strategy G requires the prosthesis users to recognize specific electrotactile modalities (e.i., vibration/pressure with different intensities), rather than only need to discriminate the intensity/frequency changes with strategies LA, LF and B. Strategies LA, LF and B are able to be used for BSDT with similar efficiency since the discrimination time includes stiffness discrimination and transfer time. Nevertheless, electrotactile feedback with suitable encoding strategies appears to be a viable approach for object stiffness recognition, which may be sufficient for a wide range of functional tasks.

The practicability of electrotactile feedback also can be evidenced by the trends of *CDR*s and the discrimination time over sequential number of test trials (Fig. 6). Our results displayed that after experienced the first 3 test trials, all the four kinds of *CDR*s and the discrimination time could be obviously improved to relative-steady high levels and gradually decreased to the plateau, respectively. It manifests that electrotactile feedback with current encoding strategies can be easily interpreted by the users and effectively integrated into the sensorimotor control for object stiffness discrimination without long-term training. However, if the task's difficulty increased (e.g., increase the stiffness levels), the actual discrimination performance and the learning effects should be reinvestigated [42]. In addition, the self-confidence scores demonstrated that the prosthesis users were more confident to adopt the strategies LA and B to manipulate the myoelectric hand to perform the two variants of OSDT (Fig. 7).

C. Implications, Limitations and Future Work

The ability to feel and regulate grip force of a prosthetic hand while handling objects and recognize the physical properties (e.i., object size/stiffness) is one of the most important aspect of sensory feedback for amputees [6], [7], [12]. The current study demonstrates the feasibility of electrotactile feedback is capable of functionally restoring the sensory feedback of myoelectric hands. The key significance lies in that it provides an alternative feedback approach for most of the amputees who are unable or unwilling to accept the surgery for intraneural stimulation feedback [18], [19]. From an application perspective, strategy LA should be applied preferably for different levels of grip force control due to the higher intensity discriminability. With acceptable accuracy, strategy B is better suitable for fragile object handling or efficient discrimination of different object properties (such as, size, stiffness, etc). Furthermore, for more complex functional tasks (e.g., identifying object sizes and stiffness simultaneously, etc), both the aperture angle and grip force of a myoelectric hand can be concurrently delivered to its users in the form of electrotactile feedback through multiple electrotactile interfaces, using the current (single or hybrid) encoding strategies. The actual performance of the prosthetic hand deserves to be comprehensively investigated by quantifying the optimal stimulation parameters.

One limitation of this study is that the control experiments are not conducted through intraneural tactile feedback due to lack of eligible amputees. In addition, it should be mentioned that we only used the final grip force applied on the surface of deformative objects to encode the object stiffness. However, the actual stiffness discrimination should take grip force and object deformation into consideration. Object deformation encoded by the aperture angle of the myoelectric hand also should be applied for stiffness discrimination in further investigations.

In the follow-up study, more amputee subjects will be recruited, and a daily-use bidirectional myoelectric hand integrating EMG sensors, pressure and angle sensors [43], embedded electrical micro-stimulator [44] and custom-made multi-electrode array will be tailored for each amputee user in practical use. Based on it, a battery of clinically-relevant experiments (such as, stacking cups test (SCT) and pick and lift test (PLT) [14], [15], object size and stiffness recognition [18] and distributed force control (ability to modulate grip force) [18], [45], etc.) with varied difficulty levels (e.g., everyday objects with multiple size and stiffness, different distraction task, etc) on various scenarios (e.i., with/without visual feedback) will be designed to comprehensively investigate the benefits of electrotactile feedback on the myoelectric hands. Furthermore, due to sEMG control accuracy and electrotactile feedback can jointly affect the performance of a myoelectric hand [2], [18], [19], we will test the influence of different sEMG control algorithms [46], [47] on the overall performance of a closed-loop myoelectric hand, and the interference problem between sEMG and electrotactile stimulation also will be investigated through dynamic blanking of stimulation artifacts [48].

References

[1] P. Geethanjali, "Myoelectric control of prosthetic hands: State-of-the-art review," *Med. Devices*, vol. 9, p. 247, Jul. 2016.

[2] D. Yang, Y. Gu, N. V. Thakor, and H. Liu, "Improving the functionality, robustness, and adaptability of myoelectric control for dexterous motion restoration," *Exp. Brain Res.*, vol. 237, no. 2, pp. 291–311, Feb. 2019.

[3] E. Biddiss and T. Chau, "Upper-limb prosthetics: Critical factors in device abandonment," *Amer. J. Phys. Med. Rehabil.*, vol. 86, no. 12, pp. 977–987, 2007.

[4] K. Østlie, I. M. Lesjø, R. J. Franklin, B. Garfelt, O. H. Skjeldal, and P. Magnus, "Prosthesis rejection in acquired major upper-limb amputees: A population-based survey," *Disab. Rehabil. Assist. Technol.*, vol. 7, no. 4, pp. 294–303, 2012.

[5] P. Svensson, U. Wijk, A. Björkman, and C. Antfolk, "A review of invasive and non-invasive sensory feedback in upper limb prostheses," *Exp. Rev. Med. Devices*, vol. 14, no. 6, pp. 439–447, Jun. 2017.

[6] J. W. Sensinger and S. Dosen, "A review of sensory feedback in upper-limb prostheses from the perspective of human motor control," *Frontiers Neurosci.*, vol. 14, p. 345, Jun. 2020.

[7] J. A. George *et al.*, "Biomimetic sensory feedback through peripheral nerve stimulation improves dexterous use of a bionic hand," *Sci. Robot.*, vol. 4, no. 32, Jul. 2019, Art. no. eaax2352.

[8] B. Rosén, H. H. Ehrsson, C. Antfolk, C. Cipriani, F. Sebelius, and G. Lundborg, "Referral of sensation to an advanced humanoid robotic hand prosthesis," *Scandin. J. Plastic Reconstructive Surgery Hand Surgery*, vol. 43, no. 5, pp. 1–7, 2009.

[9] D. M. Page *et al.*, "Motor control and sensory feedback enhance prosthesis embodiment and reduce phantom pain after long-term hand amputation," *Frontiers Hum. Neurosci.*, vol. 12, p. 352, Sep. 2018.

[10] C. Dietrich *et al.*, "Sensory feedback prosthesis reduces phantom limb pain: Proof of a principle," *Neurosci. Lett.*, vol. 507, no. 2, pp. 97–100, Jan. 2012.

[11] J. S. Schofield, K. R. Evans, J. P. Carey, and J. S. Hebert, "Applications of sensory feedback in motorized upper extremity prosthesis: A review," *Exp. Rev. Med. Devices*, vol. 11, no. 5, pp. 499–511, Jun. 2014.

[12] S. J. Bensmaia, D. J. Tyler, and S. Micera, "Restoration of sensory information via bionic hands," *Nature Biomed. Eng.*, 2020, doi: 10.1038/s41551-020-00630-8.

[13] S. Micera, J. Carpaneto, and S. Raspopovic, "Control of hand prostheses using peripheral information," *IEEE Rev. Biomed. Eng.*, vol. 3, pp. 48–68, 2010.

[14] E. Mastinu *et al.*, "Grip control and motor coordination with implanted and surface electrodes while grasping with an osseointegrated prosthetic hand," *J. NeuroEng. Rehabil.*, vol. 16, no. 1, pp. 1–10, Dec. 2019.

[15] F. Clemente *et al.*, "Intraneural sensory feedback restores grip force control and motor coordination while using a prosthetic hand," *J. Neural Eng.*, vol. 16, no. 2, Apr. 2019, Art. no. 026034.

[16] T. J. Arakeri, B. A. Hasse, and A. J. Fuglevand, "Object discrimination using electrotactile feedback," *J. Neural Eng.*, vol. 15, no. 4, Aug. 2018, Art. no. 046007.

[17] L. Vargas, H. Shin, H. H. Huang, Y. Zhu, and X. Hu, "Object stiffness recognition using haptic feedback delivered through transcutaneous proximal nerve stimulation," *J. Neural Eng.*, vol. 17, no. 1, Dec. 2019, Art. no. 016002.

[18] E. D'Anna *et al.*, "A closed-loop hand prosthesis with simultaneous intraneural tactile and position feedback," *Sci. Robot.*, vol. 4, no. 27, Feb. 2019, Art. no. eaau8892.

[19] M. A. Schiefer, E. L. Graczyk, S. M. Sidik, D. W. Tan, and D. J. Tyler, "Artificial tactile and proprioceptive feedback improves performance and confidence on object identification tasks," *PLoS ONE*, vol. 13, no. 12, Dec. 2018, Art. no. e0207659.

[20] C. M. Oddo *et al.*, "Intraneural stimulation elicits discrimination of textural features by artificial fingertip in intact and amputee humans," *Elife*, vol. 5, Mar. 2016, Art. no. e09148.

[21] L. Vargas, H. Huang, Y. Zhu, and X. Hu, "Object shape and surface topology recognition using tactile feedback evoked through transcutaneous nerve stimulation," *IEEE Trans. Haptics*, vol. 13, no. 1, pp. 152–158, Jan. 2020.

[22] A. Mazzoni *et al.*, "Morphological neural computation restores discrimination of naturalistic textures in trans-radial amputees," *Sci. Rep.*, vol. 10, no. 1, pp. 1–14, Dec. 2020.

[23] D. S. Childress, "Closed-loop control in prosthetic systems: Historical perspective," *Ann. Biomed. Eng.*, vol. 8, nos. 4–6, pp. 293–303, Jul. 1980.

[24] M. A. Wilke, C. Hartmann, F. Schimpf, D. Farina, and S. Dosen, "The interaction between feedback type and learning in routine grasping with myoelectric prostheses," *IEEE Trans. Haptics*, vol. 13, no. 3, pp. 645–654, Jul. 2019.

[25] S. Marco *et al.*, "Hand synergies: Integration of robotics and neuroscience for understanding the control of biological and artificial hands," *Phys. Life Rev.*, vol. 17, pp. 1–23, Jul. 2016.

[26] A. E. Pena, L. Rincon-Gonzalez, J. J. Abbas, and R. Jung, "Effects of vibrotactile feedback and grasp interface compliance on perception and control of a sensorized myoelectric hand," *PLoS ONE*, vol. 14, no. 1, Jan. 2019, Art. no. e0210956.

[27] F. Clemente, M. D'Alonzo, M. Controzzi, B. B. Edin, and C. Cipriani, "Non-invasive, temporally discrete feedback of object contact and release improves grasp control of closed-loop myoelectric transradial prostheses," *IEEE Trans. Neural Syst. Rehabil. Eng.*, vol. 24, no. 12, pp. 1314–1322, Dec. 2015.

[28] R. S. Johansson and J. R. Flanagan, "Coding and use of tactile signals from the fingertips in object manipulation tasks," *Nature Rev. Neurosci.*, vol. 10, no. 5, pp. 345–359, 2009.

[29] G. Valle *et al.*, "Hand control with invasive feedback is not impaired by increased cognitive load," *Frontiers Bioeng. Biotechnol.*, vol. 8, p. 287, Apr. 2020.

[30] Y. Ban, T. Narumi, T. Tanikawa, and M. Hirose, "Controlling perceived stiffness of pinched objects using visual feedback of hand deformation," in *Proc. IEEE Haptics Symp. (HAPTICS)*, Feb. 2014, pp. 557–562.

[31] V. C. Paulun, F. Schmidt, J. J. R. van Assen, and R. W. Fleming, "Shape, motion, and optical cues to stiffness of elastic objects," *J. Vis.*, vol. 17, no. 1, p. 20, Jan. 2017.

[32] F. Schmidt, V. C. Paulun, J. J. R. van Assen, and R. W. Fleming, "Inferring the stiffness of unfamiliar objects from optical, shape, and motion cues," *J. Vis.*, vol. 17, no. 3, p. 18, Mar. 2017.

[33] H. J. Witteveen, F. Luft, J. S. Rietman, and P. H. Veltink, "Stiffness feedback for myoelectric forearm prostheses using vibrotactile stimulation," *IEEE Trans. Neural Syst. Rehabil. Eng.*, vol. 22, no. 1, pp. 53–61, Jan. 2013.

[34] L. Vargas, H. Huang, Y. Zhu, and X. Hu, "Stiffness perception using transcutaneous electrical stimulation during active and passive prosthetic control," in *Proc. 42nd Annu. Int. Conf. IEEE Eng. Med. Biol. Soc. (EMBC)*, Jul. 2020, pp. 3909–3912.

[35] G. Valle *et al.*, "Biomimetic intraneural sensory feedback enhances sensation naturalness, tactile sensitivity, and manual dexterity in a bidirectional prosthesis," *Neuron*, vol. 100, no. 1, pp. 37–45, Oct. 2018.

[36] J. S. Schofield, C. E. Shell, D. T. Beckler, Z. C. Thumser, and P. D. Marasco, "Long-term home-use of sensory-motor-integrated bidirectional bionic prosthetic arms promotes functional, perceptual, and cognitive changes," *Frontiers Neurosci.*, vol. 14, p. 120, Feb. 2020.

[37] D. T. Beckler, Z. C. Thumser, J. S. Schofield, and P. D. Marasco, "Using sensory discrimination in a foraging-style task to evaluate human upper-limb sensorimotor performance," *Sci. Rep.*, vol. 9, no. 1, pp. 1–19, Dec. 2019.

[38] N. Prins *et al.*, *Psychophysics: A Practical Introduction*. New York, NY, USA: Academic, 2016.

[39] H. L. Blackburn and A. L. Benton, "Revised administration and scoring of the digit span test," *J. Consulting Psychol.*, vol. 21, no. 2, pp. 139–143, 1957.

[40] G. Valle *et al.*, "Sensitivity to temporal parameters of intraneural tactile sensory feedback," *J. NeuroEng. Rehabil.*, vol. 17, no. 1, pp. 1–12, Dec. 2020.

[41] G. Valle *et al.*, "Comparison of linear frequency and amplitude modulation for intraneural sensory feedback in bidirectional hand prostheses," *Sci. Rep.*, vol. 8, no. 1, pp. 1–13, Dec. 2018.

[42] G. Chai, D. Zhang, and X. Zhu, "Developing non-somatotopic phantom finger sensation to comparable levels of somatotopic sensation through user training with electrotactile stimulation," *IEEE Trans. Neural Syst. Rehabil. Eng.*, vol. 25, no. 5, pp. 469–480, May 2017.

[43] G. Chai, J. Briand, S. Su, X. Sheng, and X. Zhu, "Electrotactile feedback with spatial and mixed coding for object identification and closed-loop control of grasping force in myoelectric prostheses," in *Proc. 41st Annu. Int. Conf. IEEE Eng. Med. Biol. Soc. (EMBC)*, Jul. 2019, pp. 1805–1808.

[44] H. Wang, G. Chai, X. Sheng, and X. Zhu, "A programmable, multichannel, miniature stimulator for electrotactile feedback of neural hand prostheses," in *Proc. 10th Int. IEEE/EMBS Conf. Neural Eng. (NER)*, May 2021, pp. 1026–1029.

[45] Z. C. Thumser, A. B. Slifkin, D. T. Beckler, and P. D. Marasco, "Fitts' law in the control of isometric grip force with naturalistic targets," *Frontiers Psychol.*, vol. 9, p. 560, Apr. 2018.

[46] C. Chen, G. Chai, W. Guo, X. Sheng, D. Farina, and X. Zhu, "Prediction of finger kinematics from discharge timings of motor units: Implications for intuitive control of myoelectric prostheses," *J. Neural Eng.*, vol. 16, no. 2, Apr. 2019, Art. no. 026005.

[47] J. A. George, T. S. Davis, M. R. Brinton, and G. A. Clark, "Intuitive neuromyoelectric control of a dexterous bionic arm using a modified Kalman filter," *J. Neurosci. Methods*, vol. 330, Jan. 2020, Art. no. 108462.

[48] M. A. Garenfeld *et al.*, "A compact system for simultaneous stimulation and recording for closed-loop myoelectric control," *J. NeuroEng. Rehabil.*, vol. 18, no. 1, pp. 1–17, Dec. 2021.